Old Carbon, New Insights: Thermal Reactivity and Bioavailability of Saltmarsh Soils

Alex Houston[1], Mark H Garnett[2], and William E N Austin[1,3]

1. Department of Geography and Sustainable Development, University of St Andrews, St Andrews, KY16 9AL, United Kingdom
2. NEIF Radiocarbon Laboratory, Scottish Universities Environmental Research Centre, East Kilbride, G75 0QF, United Kingdom
3. Scottish Association of Marine Science, Oban, PA37 1QA, United Kingdom

Correspondence to: Alex Houston (ah383@st-andrews.ac.uk)

Abstract

Saltmarshes are globally important coastal wetlands which can help to mitigate the impacts of climate change. They accumulate organic carbon from both modern and aged sources through in-situ biological production and the capture of ex-situ sources which are deposited during tidal inundation. Previous studies have found that long-term organic carbon storage in saltmarsh soils is driven by the net contribution from the older fraction, implying that the inputs of young organic carbon derived from in situ production are recycled at a faster rate.

Using ramped oxidation, we assessed the composition (^{14}C and ^{13}C) of saltmarsh soil carbon pools defined by their thermal reactivity. By relating ^{14}C measurements of the soil carbon pools to CO_2 respired in aerobic incubations of the same soils, we provide the first empirical evidence linking the thermal reactivity of saltmarsh soil organic carbon with its bioavailability for remineralization.

We found that old (^{14}C-depleted) carbon dominates the thermally recalcitrant organic carbon pools, whereas the thermally labile carbon is composed of younger organic carbon sources. In most cases, the ^{14}C content of the most thermally labile carbon pool was closest to the previously reported ^{14}C content of the CO_2 evolved from aerobic incubations of the same soils, implying that the bioavailability of saltmarsh soil organic carbon to remineralisation in oxic conditions is closely related to its thermal lability.

Our results highlight the importance of saltmarshes as stores of both old, thermally recalcitrant organic carbon, as well as younger, thermally labile organic carbon that is vulnerable to decomposition under oxic conditions. Management interventions (e.g. rewetting by tidal inundation)

to limit the exposure of saltmarsh soils to elevated oxygen availability may help to protect and conserve these stores of thermally labile organic carbon and hence limit CO_2 emissions. We also present the first evidence to support the inclusion of thermally labile allochthonous OC stored in saltmarsh soils in additionality assessments, with relevance to international carbon crediting projects and National GHG Inventories.

Graphical Abstract

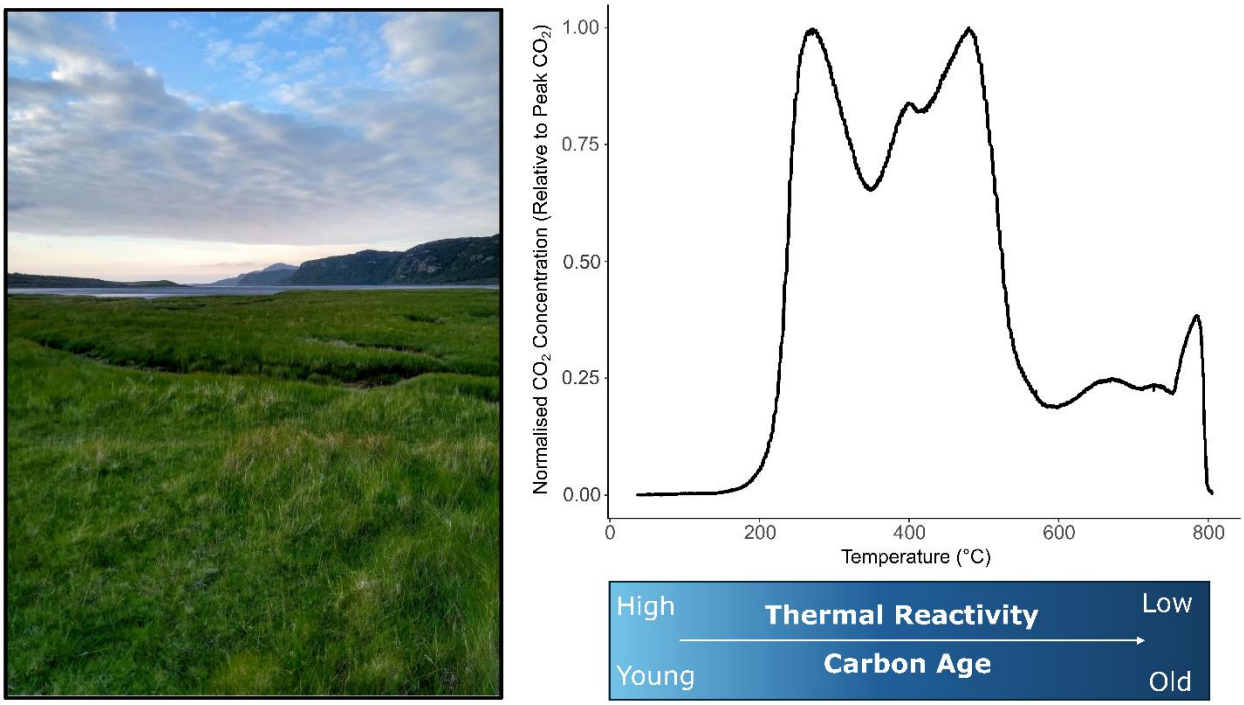

1. Introduction

Saltmarshes accumulate organic carbon (OC) of variable age and reactivity into their soils. A portion of this OC is stored for millennia, providing a climate regulation service, and some is returned to the atmosphere or laterally exported (Komada et al., 2022; Macreadie et al., 2021). Saltmarshes also accumulate and produce inorganic carbon (IC) but the climate regulation service of this is currently under debate and unclear (Granse et al., 2024; Van Dam et al., 2021).

To understand the role of saltmarsh soils in carbon cycling and their potential for climate mitigation through targeted management interventions, much research has focussed on determining the autochthonous (in-situ) and allochthonous (ex-situ, trapped during tidal inundation from terrestrial and marine sources) contributions to saltmarsh soils, with the accumulation of autochthonous OC as a direct sequestration of carbon from the atmosphere, reducing the amount of atmospheric greenhouse gases (GHGs) (Macreadie et al., 2019; Saintilan et al., 2013; Van de Broek et al., 2018). The accumulation of allochthonous OC, originally sequestered outside the saltmarsh area, does not directly reduce atmospheric GHGs, but can represent a source of avoided emissions if it remains stored in the saltmarsh soil for longer than in an alternative depositional environment (Howard et al., 2023). Evidence to determine whether this is the case or not, and under what scenarios, has proven challenging to obtain (Geraldi et al., 2019; Houston et al., 2024a). OC pools with distinct biological turnover times may instead provide greater insights into the soil carbon residence time and therefore the climate mitigation achieved through targeted management interventions to retain that carbon (Sanderman and Grandy, 2020).

Ramped oxidation (RO) and ramped pyrolysis oxidation (RPO) have been used to estimate the thermal reactivity and biological turnover time of soil and sediment OC (Hemingway et al., 2017b; Plante et al., 2011; Rosenheim et al., 2008). RO and RPO involve measuring the quantity of CO_2 evolved as a sample is increasingly heated at a constant rate in an atmosphere containing oxygen (e.g., Plante et al., 2011; Stoner et al., 2023), or other gases, typically Helium (RPO: e.g., Hemingway et al., 2017a; Rosenheim et al., 2008). The temperature at which CO_2 is thermally-evolved is related to the activation energy required to thermally decompose C (Hemingway et al., 2017b), which is also an estimate of the energy required for biological degradation of OC (Peltre et al., 2013; Plante et al., 2013). CO_2 evolved at low temperatures is deemed to be from soil OC pools with a greater thermal lability than CO_2 evolved at higher temperatures (Peltre et al., 2013; Rosenheim et al., 2008). OC thermal reactivity pools can be examined by collecting the evolved CO_2 from set temperature ranges with distinct thermal reactivities and measuring the ^{14}C (age)

and ^{13}C content (Rosenheim et al., 2008), which can then be related to the activation energy required to thermally decompose those C sources (Hemingway et al., 2017b).

The ^{14}C content of the thermal reactivity pools provides insight into the turnover time of each pool, with past research showing that the oldest soil organic matter (OM) (most depleted ^{14}C content) tends to dominate the most thermally recalcitrant fractions (Bao et al., 2019b; Plante et al., 2013; Stoner et al., 2023). Similar results have been found for saltmarsh soils (Luk et al., 2021). Young OC, which can be autochthonous or allochthonous (Van de Broek et al., 2018), has been found to turnover at a faster rate than old OC in saltmarsh soils (Komada et al., 2022; Van de Broek et al., 2018), implying that young OC may tend to be more thermally labile than old OC for saltmarsh soils.

The ^{13}C content of the thermal reactivity pools can also provide insight as to whether the source of OC has an influence on turnover time. Previous work has found that the ^{13}C content of evolved CO_2 tends to be more enriched at higher temperatures due to greater contributions from ^{13}C-enriched, degraded/microbially derived OC (Luk et al., 2021; Sanderman and Grandy, 2020; Stoner et al., 2023). Similarly, comparisons of the isotopic composition of thermally-defined OC pools to their chemical properties have found that thermally labile OC is derived from mostly lipids and polysaccharides, whereas OC with a higher thermal recalcitrance is derived from a greater proportion of phenolic and aromatic compounds (Sanderman and Grandy, 2020). The thermal reactivity of soil and sediment OC is also influenced by the formation of organo-mineral complexes, which can physically and chemically stabilise OC (Bianchi et al., 2024; Hemingway et al., 2019). Mineral-associations can increase the energy required for decomposition and have been found to increase thermal recalcitrance and to slow turnover times of soil and sediment OC (Hemingway et al., 2019; Stoner et al., 2023).

Crucially, the biological availability (bioavailability) of OC for decomposition, and hence its biological turnover time, depends on the prevailing environmental conditions as well as thermal reactivity (Hemingway et al., 2017b; Schmidt et al., 2011). For example, increased hydrodynamic energy can destabilise organo-mineral complexes and increase the bioavailability of previously stable OC (Spivak et al., 2019). Similarly, increased oxygen availability can decrease the energy requirement for microbes to decompose molecularly recalcitrant OC, causing it to be remineralised at a faster rate (Noyce et al., 2023).

Houston et al. (2024b) found that young OC stored in saltmarsh soils was preferentially respired as carbon dioxide (CO_2) during aerobic incubation experiments, but that a portion of the respired CO_2 was produced from an aged (^{14}C-depleted), allochthonous source. It is possible that this

CO_2 could have been respired from thermally labile as well as thermally recalcitrant soil OC sources because the increased oxygen availability of the incubations potentially facilitated the degradation of OC which was previously stable in the low-oxygen environment of typical saltmarsh soils (Noyce et al., 2023).

The isotopic composition of RO thermal reactivity fractions can be compared to the isotopic composition of the CO_2 that is evolved biologically during incubations of equivalent samples to determine whether or not the age of the most biologically- and thermally-reactive OC pools match. Here, we present the first measurements of the ^{13}C and ^{14}C content of CO_2 derived from saltmarsh soils using RO, and the first comparison of these to the ^{14}C content of biologically evolved CO_2 from the same soils (Houston et al., 2024b). We hypothesised that the thermally labile C pools would be composed of younger C than the thermally recalcitrant pools, and that the CO_2 evolved from saltmarsh soils exposed to oxic conditions (Houston et al., 2024b) are from a predominantly thermally labile OC pool.

2. Methods

2.1. Field site and sample collection

Three saltmarsh soil cores (T1-3) were retrieved ca. 30 m apart from the lower marsh zone from Skinflats (SK), an estuarine saltmarsh in Scotland (56° 3'34.04"N, 3°43'59.16"W), as detailed in Houston et al. (2024b). Field methods and laboratory sub-sampling procedures are described in detail in Houston et al. (2024b). Briefly, the cores were split into 1 cm thick slices as follows: core T1 (0-1 cm, 5-6 cm, and 18-19 cm); T2 (0-1 cm, 5-6 cm, and 15-16 cm), and T3 (0-1 cm, 5-6 cm, and 19-20 cm) (with the deepest sample from each core being the deepest retrieved sample from the 20 cm length of the corer. On the occasions when a full core was not retrieved, the deepest retrieved soil was used). Each slice was subsequently divided to provide sample material for the RO procedure, and for aerobic laboratory incubations from which the biologically evolved CO_2 was collected for ^{13}C and ^{14}C analysis (Houston et al., 2024b).

2.2. Ramped oxidation

The RO sub-samples were individually dried to constant mass before milling to a fine powder to homogenise and limit potential shielding effects from aggregates. Unlike most RO and RPO studies (e.g., Hemingway et al., 2017b), we did not remove carbonates from our samples. Acid treatment, which is required to remove carbonates from samples has been demonstrated to result in losses from the labile OC fraction (Bao et al., 2019a). A loss of labile OC for our samples could seriously impact the interpretations in our study, and our ability to compare the ^{14}C content

of the CO_2 respired from bulk (untreated) soils in the incubation experiments (Houston et al., 2024b) to the ^{14}C content of the RO thermal fractions.

The samples were sent to the NEIF Radiocarbon Laboratory for RO, which is described in Garnett et al. (2023). The RO procedure involved two stages, a first combustion to determine the relationship between the rate of CO_2 evolution and temperature (thermogram), and a second combustion where evolved sample gases were collected across defined temperature ranges, for subsequent isotope analysis. For the first combustion, ca. 200 mg of dried and homogenized sample material was weighed into a quartz vial which was inset into a quartz combustion tube, which was subsequently placed into a furnace set initially to room temperature. The furnace was progressively heated at a constant rate of 5°C per minute to 800°C in a stream of high purity oxygen (N5.5, BOC, UK). Heating caused combustion of the sample and the evolution of gas which was passed into a second quartz combustion tube containing platinised wool in a furnace set to a constant temperature of 950°C. The platinised wool acted as a catalyst to ensure complete combustion of the evolved gases. Upon exiting the secondary combustion chamber the sample passed through a glass tube containing magnesium perchlorate desiccant to remove moisture and subsequently the CO_2 concentration of the gas was measured using a non-dispersive infrared CO_2 sensor (SprintIR®-WF-5, Gas Sensing Solutions, UK). The sample was then passed out of the sensor unit and vented to the atmosphere.

The measured CO_2 concentration (normalised for sample mass) was plotted against temperature to produce thermograms which were used to identify temperature ranges, which defined C thermal reactivity pools for this study: 150-325 °C, 325-425 °C, 425-500 °C,500-650 °C, and 650-800 °C.

For each sample, the required mass of material to evolve sufficient CO_2 (> 3 mL) for ^{14}C measurement was calculated based on the thermogram. A new sub-set from the original dried and homogenised sample was then re-run following the RO procedure outlined above, but instead of venting to atmosphere, after its measurement the evolved CO_2 was collected into foil gas bags based on the defined temperature ranges. CO_2 was collected for ^{13}C analysis from 650-800 °C, but sufficient CO_2 was evolved for ^{14}C analysis from this thermal fraction for only one sample (T1 0.5 cm, Table A1) and we do not consider this fraction further because it is likely dominated by carbonates and not relevant to the purpose of this study.

The foil gas bags (5 L Spout Pouch, https://www.pouchshop.co.uk/) used for sample collection were sealed with one-hole rubber bungs into which a 0.6 cm diameter x 5 cm length stainless steel tube was inserted. Isoversinic tubing (Saint Gobain, France) was fitted over the stainless

steel to connect it to a quick coupling (Colder Products Company, USA), which allowed connection to the RO kit.

Prior to the RO CO_2 collection, all equipment was cleaned using a standardised procedure (Garnett et al., 2023). All glassware was combusted at 900°C for a minimum of two hours, and all couplings and connectors were washed in carbon-free detergent (Decon) and rinsed in Milli-Q water. The foil gas bags were cleaned by repeatedly (3 times) filling with ca. 1 L high purity nitrogen gas (Research Grade 99.9995% purity, BOC, UK) and evacuating with an air pump, over a period of at least 24 hours (to aid out-gassing of CO_2). The final evacuation, immediately before connecting to the RO rig, involved pumping out the bags with an SBA-5 CO_2 analyser (PPsystems, USA) to ensure that the bags did not contain significant contamination. Before commencing a sample combustion, the entire RO rig was checked for leaks and other potential sources of contamination by measuring the CO_2 concentration in the oxygen carrier gas exiting the kit, using the SBA-5 CO_2 analyser.

Within 3 days of combusting a sample, the evolved gas in each foil bag was connected to a vacuum rig for cryogenic recovery of pure sample CO_2 by passing it through slush (–78ºC; dry ice and industrial methylated spirits) and then liquid nitrogen (–196ºC) traps, under high vacuum (ca. 3×10^{-3} millibars). The sample CO_2 was then split into three aliquots: One for $\delta^{13}C$ analysis using isotope ratio mass spectrometry (IRMS; Delta V, Thermo-Fisher, Germany), one for graphitisation and subsequent AMS ^{14}C analysis, and one for an archive back-up. The graphitised AMS samples were measured for ^{14}C content at the SUERC AMS Laboratory (see Ascough et al., 2024). The ^{13}C content ($\delta^{13}C$-VPDB) was used to normalise the ^{14}C results to a $\delta^{13}C$ of -25 ‰ to correct for isotopic fractionation. Following convention, ^{14}C results are presented as %Modern (fraction modern x 100) and conventional radiocarbon ages (years BP, where 0 BP = AD 1950 and age = -8033 x Ln (%Modern/100)).

2.3. Data Analysis

Continuous activation energy distributions were modelled from thermograms using the '*rampedpyrox*' package in Python V3.8 (Hemingway, 2016; Hemingway et al., 2017b). The *rampedpyrox* model calculates mean activation energies (μE) and the standard deviation of activation energy (σE), which is a measure of the heterogeneity of bond strength, for each temperature fraction which CO_2 was collected from. Mean μE, σE and activation energy distribution (p (o,E)) are also calculated for each sample using the *rampedpyrox* model. We do not use the *rampedpyrox* model for calculation of isotope values as it applies a blank correction to ^{14}C (Hemingway et al., 2017a, b) which is not relevant to the analytical set-up for this study

(Garnett et al., 2023), and the ^{13}C values generated varied significantly from our IRMS measured values (Table A2). Further data analysis and visualisation of thermograms and isotopic data was undertaken using RStudio V4.2.2 (R Core Team, 2022).

3. Results

3.1. Radiocarbon

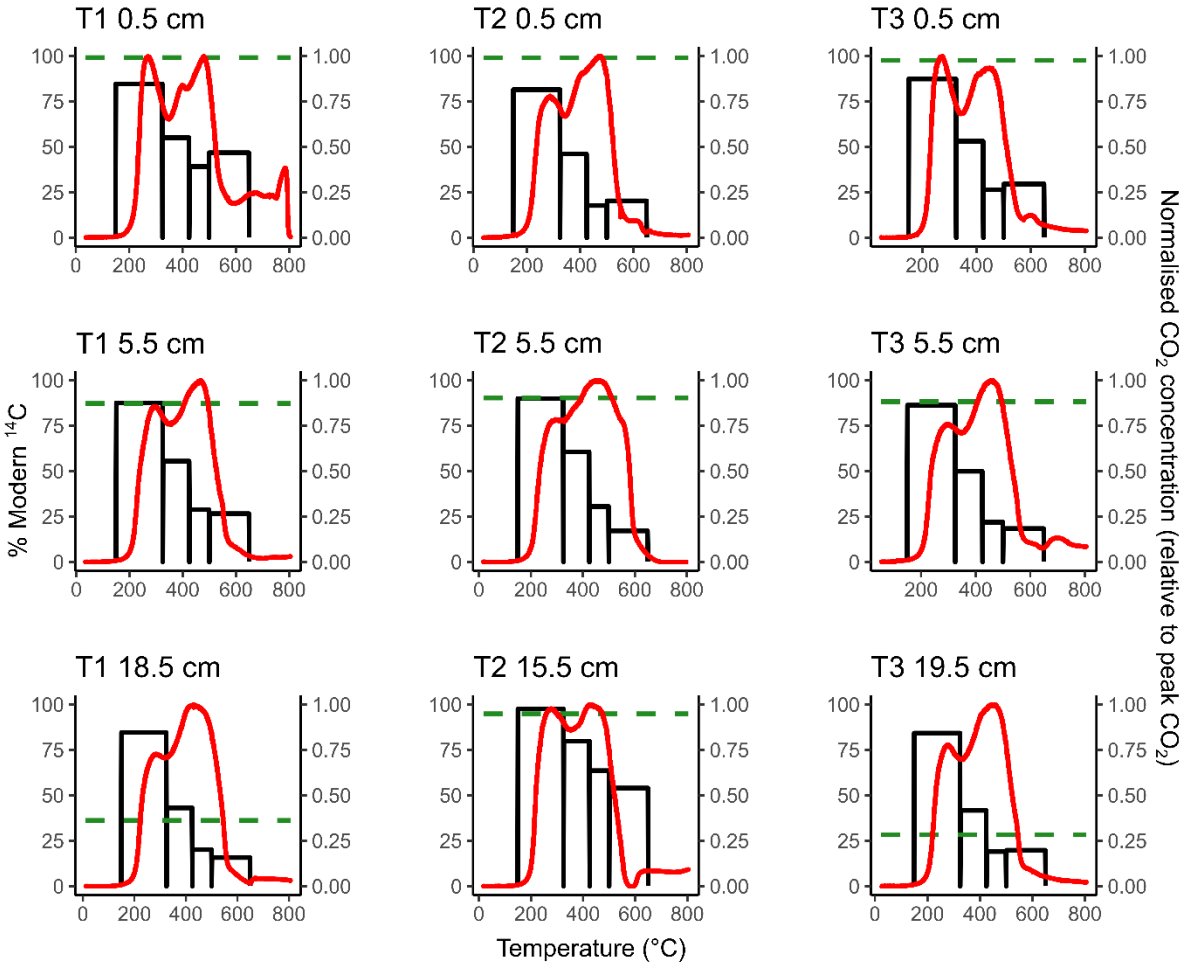

Figure 1. Thermograms (red lines, right-hand y-axis) overlaying the ^{14}C content of ramped oxidation fractions (black bars, left-hand y-axis) for each sample. The horizontal green dashed lines represent the ^{14}C content of the CO_2 respired from the aerobic incubation experiments of Houston et al. (2024b).

The ^{14}C content of the RO fractions (Fig. 1, Table 1) were statistically similar between the 0.5 cm, 5.5 cm, and deepest sample (T1 18.5 cm, T2 15.5 cm, T3 19.5 cm) depth increments for each of the temperature fractions (Kruskal-Wallis; p = 0.83, 0.38, 0.66, 0.99, for 150-325°C, 325- 425°C, 425-500°C, 500-650°C, respectively). There were, however, clear differences in ^{14}C contents between the temperature fractions, with ranges of 81.50-97.54 % Modern for 150-325 °C, 41.67-

79.80 % Modern for 325-425 °C, 17.67-63.56 % Modern for 425-500 °C, and 15.69-53.96 % Modern for 500-650 °C (Fig. 1, Table 1).

Table 1. Radiocarbon concentration (% Modern) of RO temperature fractions and the CO_2 produced in soil incubation experiments in Houston et al. (2024b). Errors are reported to one standard deviation from the mean. A sole ^{14}C measurement for T1 0.5 cm 650-800 °C is reported in Table A1.

	% Modern ^{14}C				
	150-325°C	**325-425°C**	**425-500°C**	**500-650°C**	**Incubation CO_2 (Houston et al., 2024b)**
T1 0.5 cm	84.62 ± 0.44	55.02 ± 0.29	39.18 ± 0.21	46.75 ± 0.26	99.15 ± 0.45
T1 5.5 cm	87.51 ± 0.43	55.43 ± 0.28	28.76 ± 0.17	26.56 ± 0.16	87.18 ± 0.38
T1 18.5 cm	84.56 ± 0.44	43.06 ± 0.23	20.07 ± 0.13	15.70 ± 0.12	36.13 ± 0.36
T2 0.5 cm	81.50 ± 0.43	46.04 ± 0.24	17.67 ± 0.13	20.26 ± 0.14	98.97 ± 0.43
T2 5.5 cm	89.95 ± 0.42	60.55 ± 0.30	30.54 ± 0.17	17.11 ± 0.12	90.26 ± 0.40
T2 15.5 cm	97.53 ± 0.50	79.80 ± 0.41	63.56 ± 0.31	53.96 ± 0.27	94.86 ± 0.44
T3 0.5 cm	87.37 ± 0.45	53.09 ± 0.28	26.37 ± 0.15	29.55 ± 0.17	97.56 ± 0.43
T3 5.5 cm	86.23 ± 0.42	49.86 ± 0.25	21.87 ± 0.14	18.36 ± 0.12	88.22 ± 0.41
T3 19.5 cm	84.23 ± 0.41	41.67 ± 0.22	19.04 ± 0.13	19.76 ± 0.14	28.25 ± 0.37

3.2. $\delta^{13}C$

There were no significant differences in the ^{13}C content of the ramped oxidation fractions (Fig. 2, Table 2) between the depth increments (Kruskal-Wallis; p = 0.66, 0.63, 0.63, 0.44, 0.17, for 150-325 °C, 325-400 °C, 425-500 °C, 500-650 °C, 650-800 °C respectively). ^{13}C contents followed the opposite trend to ^{14}C contents with temperature, with ranges of -28.0 to -24.7 ‰ for 150-325 °C, -26.6 to -22.3 ‰ for 325-425 °C, -25.4 to -20.2 ‰ for 425-500 °C, -24.4 to -13.9 ‰ for 500-650 °C, and -21.1 to -4.0 ‰ for 650-800 °C (Fig. 2, Table 2).

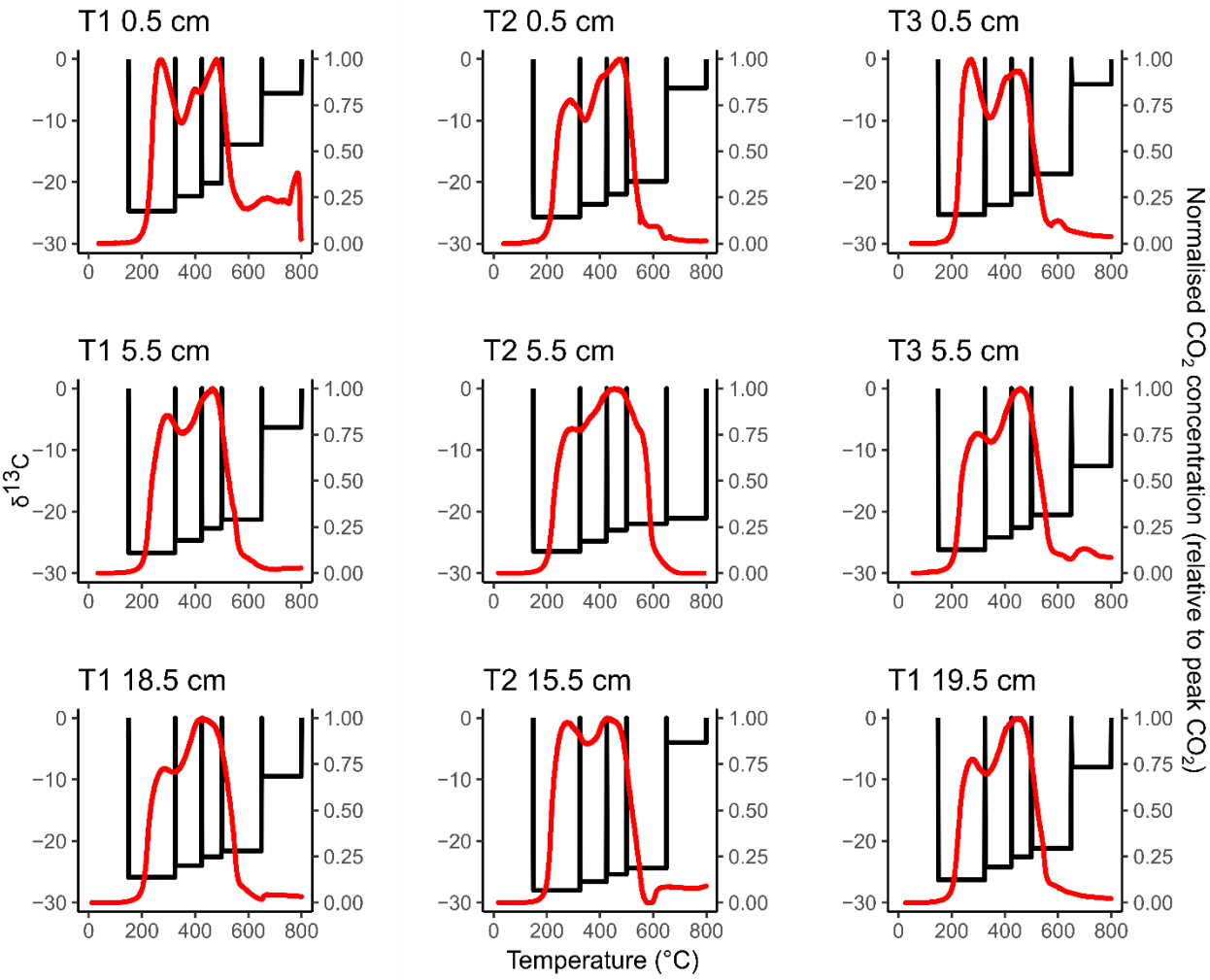

194

195 *Figure 2. Thermograms (red lines, right-hand y-axis) overlaying the ^{13}C content of the RO*
196 *temperature fractions (black bars, left-hand y-axis) for each sample. Unlike Fig. 1, we did not*
197 *attempt to relate the ^{13}C-RO to the ^{13}C content of the CO_2 respired in the incubation experiments,*
198 *due to the potential for microbial fractionation during the incubation experiments.*

199

Table 2. δ^{13}C-VPDB‰ signature of the RO temperature fractions and the incubation experiments in Houston et al. (2024b). Errors are reported to one standard deviation from the mean.

	δ^{13}C-VPDB‰					
	150-325°C	**325-425°C**	**425-500°C**	**500-650°C**	**650-800°C**	**Incubations (Houston et al., 2024b)**
T1 0.5 cm	-24.7 ± 0.1	-22.3 ± 0.1	-20.2 ± 0.1	-13.9 ± 0.1	-5.6 ± 0.1	-23.3 ± 0.1
T1 5.5 cm	-26.7 ± 0.1	-24.7 ± 0.1	-22.7 ± 0.1	-21.3 ± 0.1	-6.3 ± 0.1	-23.6 ± 0.1
T1 18.5 cm	-25.9 ± 0.1	-24.0 ± 0.1	-22.6 ± 0.1	-21.6 ± 0.1	-9.5 ± 0.1	-6.1 ± 0.1
T2 0.5 cm	-25.7 ± 0.1	-23.6 ± 0.1	-22.0 ± 0.1	-19.9 ± 0.1	-4.7 ± 0.1	-22.9 ± 0.1
T2 5.5 cm	-26.5 ± 0.1	-24.8 ± 0.1	-23.0 ± 0.1	-22.0 ± 0.1	-21.1 ± 0.1	-23.1 ± 0.1
T2 15.5 cm	-28.0 ± 0.1	-26.6 ± 0.1	-25.4 ± 0.1	-24.4 ± 0.1	-4.0 ± 0.1	-20.2 ± 0.1
T3 0.5 cm	-25.3 ± 0.1	-23.7 ± 0.1	-22.0 ± 0.1	-18.7 ± 0.1	-4.1 ± 0.1	-20.6 ± 0.1
T3 5.5 cm	-26.2 ± 0.1	-24.2 ± 0.1	-22.6 ± 0.1	-20.5 ± 0.1	-12.6 ± 0.1	-23.4 ± 0.1
T3 19.5 cm	-26.3 ± 0.1	-24.2 ± 0.1	-22.6 ± 0.1	-21.2 ± 0.1	-8.0 ± 0.1	-3.7 ± 0.1

3.3. Ramped oxidation and incubation comparison

Figure 1 presents a comparison of the ^{14}C content of the RO temperature fractions and respired CO_2 from the same soils during aerobic laboratory incubations (Houston et al. 2024b). These comparisons show that for each of the 0.5 cm depth samples, the ^{14}C content of the respired CO_2 was greater than the ^{14}C content of any of the RO temperature fractions in the same soils (Fig. 1). For the 5.5 cm depth samples, the ^{14}C content of the CO_2 respired in the incubations was approximately equivalent to the ^{14}C content of the 150-325°C RO temperature fraction (Fig. 1). For T2 15.5 cm, the ^{14}C content of the respired CO_2 was also closest to the 150-325°C RO temperature fraction (Fig. 1). For the T1 18.5 cm and T3 19.5 cm samples, the ^{14}C contents of the incubation CO_2 were depleted relative to the 150-325°C RO temperature fraction for both samples, and instead, were closest to the 325-425°C and 425-500°C RO temperature fractions, respectively (Fig. 1).

3.4. Activation Energy

Mean activation energy (μE) ranged from 157.50-170.97 kJ/mol for the 0.5 cm depth samples, 159.97-165.32 kJ/mol for the 5.5 cm depth samples, and 154.38-160.44 kJ/mol for the deepest samples (T1 18.5 cm, T2 15.5 cm, T3 19.5 cm. Table 3). The standard deviation of activation energy (σE) ranged from 23.16-35.83 kJ/mol for the 0.5 cm depth samples, 22.16-25.25 kJ/mol for the 5.5 cm depth samples, and 21.43-23.51 kJ/mol for the deepest samples (Table 3). Between the three depth increments, there were no significant changes in μE, σE, nor activation energy distribution (p (o,E) (Table 1. ANOVA; p = 0.47, 0.37, and 0.14, respectively).

Table 3. Mean activation energy (μE), standard deviation of activation energy (σE), and activation energy distribution for each sample.

	μE (kJ/mol)	σE (kJ/mol)	p (oE)
T1 0.5 cm	170.97	35.83	0.02
T1 5.5 cm	159.97	22.16	0.02
T1 18.5 cm	160.44	22.72	0.02
T2 0.5 cm	160.47	23.16	0.02
T2 5.5 cm	165.32	25.25	0.01
T2 15.5 cm	154.38	21.43	0.02
T3 0.5 cm	157.50	24.01	0.02
T3 5.5 cm	162.31	24.44	0.02
T3 19.5 cm	160.13	23.51	0.02

Table 4 shows μE and the associated σE for each thermal fraction. μE ranged from 131.04-133.23 kJ/mol for 150-325 °C, 156.83-157.78 kJ/mol for 325-425 °C, 176.14-177.79 kJ/mol for 425-500 °C, 185.44-199.19 kJ/mol for 500-650 °C, and 213.06-247.75 kJ/mol for 650-800 °C (Table 4). σE ranged from 7.33-8.71 kJ/mol for 150-325 °C, 9.83-10.23 kJ/mol for 325-425 °C, 6.88-8.83 kJ/mol for 425-500 °C, 3.68-16.04 kJ/mol for 500-650 °C, and 1.83-10.94 kJ/mol for 650-800 °C (Table 4). μE and σE both varied significantly between the thermal fractions, increasing sequentially (Kruskal-Wallis, $p = 0.001$ and 0.001, respectively). We therefore infer that the thermal recalcitrance of RO fractions is greater at higher temperatures and use temperature as a proxy for thermal reactivity herein.

Table 4. Mean activation energy (μE) and standard deviation of activation energy (σE) for each RO temperature fraction for each sample.

	μE (σE) (kJ/mol)				
	150-325°C	**325-425°C**	**425-500°C**	**500-650°C**	**650-800°C**
T1 0.5 cm	132.43 (7.33)	157.52 (10.17)	177.79 (7.32)	199.19 (16.04)	242.42 (10.94)
T1 5.5 cm	133.23 (8.07)	157.00 (10.13)	177.07 (7.58)	191.06 (7.87)	213.06 (2.12)
T1 18.5 cm	131.90 (8.62)	157.60 (9.83)	176.93 (7.83)	189.53 (6.70)	239.73 (6.73)
T2 0.5 cm	132.10 (8.21)	157.42 (10.08)	177.23 (7.38)	191.39 (10.62)	226.84 (6.81)
T2 5.5 cm	132.15 (8.71)	157.11 10.01)	177.68 (8.83)	195.80 (7.95)	224.56 (4.55)
T2 15.5 cm	131.04 (8.46)	156.83 (10.23)	176.69 (6.88)	185.44 (3.68)	247.74 (1.83)
T3 0.5 cm	131.59 (7.48)	157.33 (10.07)	176.14 (7.07)	193.65 (12.46)	231.21 (10.04)
T3 5.5 cm	133.05 (8.28)	157.67 (10.14)	177.19 (7.70)	191.13 (9.11)	236.57 (4.29)
T3 19.5 cm	131.73 (8.38)	157.78 (10.00)	176.71 (7.34)	191.7 (10.53)	232.23 (9.69)

4. Discussion

Soils are complex mixtures of many different OC sources and ages, with different vulnerabilities to decomposition and turnover. In this study, we aimed to improve our understanding of the carbon cycling of saltmarsh soils by measuring the ^{13}C and ^{14}C content of thermally-fractionated soil carbon pools, and comparing these results to the ^{14}C content of biologically evolved CO_2 from the same soils (Houston et al., 2024b).

4.1. Carbon provenance of ramped oxidation CO_2 fractions

The first three RO temperature fractions (150-325°C, 325-425°C, 425-500°C) were derived solely from OC sources, as IC begins to breakdown from ca. 550°C (Hemingway et al., 2017b). CO_2 from the 500-650°C and 650-800°C fractions may, however, have been evolved from a mix of OC and IC sources. The IC contents of the studied soils (0.11-0.48%) were low relative to OC contents (4.18-7.71%), and IC makes only 1.95-10.48% of the total soil C pool for these samples (Table A3). Wider μE ranges (mean activation energy of each thermal fraction) and increased bond strength

diversity (σE) compared to the first three RO fractions (Table 4) may have been caused by non-first order decomposition of carbonates (a form of IC) from 550 °C, as first order decomposition kinetics are a requirement for the *rampedpyrox* model (Hemingway et al., 2017b). Hemingway (pers. comm. 16/01/2025) confirmed that due to the low amounts of carbonates in these samples (Table A3) that it would be appropriate to calculate activation energies using the *rampedpyrox* model.

IC could have been removed from our saltmarsh soil samples to allow complete analysis of the soil OC pool, and many R(P)O studies have taken this approach (Bao et al., 2019b; Hemingway et al., 2017b; Luk et al., 2021; Stoner et al., 2023; Williams and Rosenheim, 2015). However, our samples have low IC contents (Table A3), and acid-treatment, which is required to remove IC from samples, can cause losses of labile OC (Bao et al., 2019a). Indeed, in Hemingway et al. (2017), acid treatment of samples prior to RO resulted in a shift of 4 % Modern ^{14}C, which could change one of our samples from having a pre-bomb ^{14}C content to a post-bomb ^{14}C content, or vice-versa. A similar shift in ^{14}C content for our samples could seriously impact the interpretations in our study, and our ability to compare the ^{14}C content of the CO_2 respired from bulk (untreated) soils in the incubation experiments (Houston et al., 2024) to the ^{14}C content of the RO fractions. The soils in the incubation experiments were also not decarbonated as the acid-treatment would have affected soil respiration processes and made the results incomparable to in-situ soil degradation processes (Houston et al., 2024b).

4.2. ^{14}C content of ramped oxidation CO_2 fractions

The ^{14}C-RO content decreased over the four thermal fractions (150-325 °C, 325-425 °C, 425-500 °C, 500-650 °C. Fig. 1), implying that ^{14}C-depleted OC had a greater thermal recalcitrance than ^{14}C-enriched OC for these saltmarsh soil samples. Since the ^{14}C content of each RO fraction was <100 % Modern (Table 1), each of the OC reactivity pools were likely to be predominantly composed of carbon sequestered from the atmosphere before the 1963 ^{14}C bomb-spike caused by atmospheric nuclear weapons testing, although we cannot completely discount some contributions from post-bomb carbon (Hajdas et al., 2021). Nevertheless, using ^{14}C content as an estimate of the age of the OC we can infer that the older (^{14}C-depleted) OC has a greater thermal recalcitrance than young OC for these samples, which is consistent with previous studies on the thermal reactivity of carbon stored in soils and sediments (e.g., Bao et al., 2019b; Luk et al., 2021; Plante et al., 2013; Stoner et al., 2023).

The results suggest inhomogeneity within at least one of the temperature fractions for each sample as, although there were no post-bomb ^{14}C contents for the incubation or RO samples

(Table 1), there is likely to be a fraction of post-bomb (post-AD1955) OC in at least one of the temperature fractions. Autochthonous OC sequestration (post-bomb) at this accreting saltmarsh (Hajdas et al., 2021; Smeaton et al., 2024) may become obscured by contributions from pre-bomb (pre-AD1955) OC. Observing the decline in ^{14}C content with increasing temperature (Fig. 1), we hypothesise that, if present, this mixing of pre- and post-bomb C most likely occurred in the 150-325°C fraction.

As the oldest (most ^{14}C-depleted) C had the greatest thermal recalcitrance (Fig. 1), this emphasises that saltmarshes accumulating greater amounts of older (^{14}C-depleted) OC will likely provide the most thermally recalcitrant OC stores, and saltmarshes accumulating greater proportions of contemporary OC, either through in-situ production or young allochthonous components, contain soil OC stores which are of greater thermal lability (Komada et al., 2022; Van de Broek et al., 2018). However, the ^{14}C contents of the lowest temperature RO fraction (81-98 % Modern; Table 1) highlight that although the thermal reactivity of OC decreases with ^{14}C content (Fig. 1), thermally labile OC can still be aged (at least hundreds of years old) for these soils. Due to the often anaerobic and non-eroding conditions of buried sediments, saltmarshes can therefore be stores of old, but thermally labile carbon. Of course, the thermal recalcitrance of OC is not necessarily related to biological turnover time, as this is also dependent on the prevailing environmental conditions (Schmidt et al., 2011; Spivak et al., 2019).

4.3. ^{13}C content of ramped oxidation CO_2 fractions

^{13}C-RO increased sequentially with the thermal fractions (Fig. 2), due to greater contributions from relatively ^{13}C-enriched C sources from the higher temperature thermal fractions. The ^{13}C-RO contents of the 150-650 °C fractions were each typical of OC sources (Leng and Lewis, 2017), whereas the ^{13}C-RO contents of the 650-800 °C fraction were mostly typical of at least a partial contribution from an IC source, with the exception of T2 5.5 cm and T3 5.5 cm (Table 2) (Brand et al., 2014; Ramnarine et al., 2012). As IC can begin to evolve from 550 °C, it is possible that a mix of OC and IC sources was present in the 500-650 °C thermal fractions.

As ^{13}C-RO increased with temperature (Fig. 2, Table 2), ^{13}C-enriched OC had a greater thermal recalcitrance than ^{13}C-depleted OC for these samples. Previous work has demonstrated that >80 % of the OC accumulating at Skinflats saltmarsh is autochthonous/terrestrial in origin (Miller et al., 2023), with limited contributions from marine OC. The thermally recalcitrant OC was potentially composed of a greater amount of OC which has undergone microbial decomposition as this process tends to enrich the degraded OC in ^{13}C (Boström et al., 2007; Etcheverría et al., 2009; Luk et al., 2021; Sanderman and Grandy, 2020; Soldatova et al., 2024; Stoner et al., 2023).

The thermally recalcitrant OC may instead/also have been composed of more different OM compounds (e.g., lignins, aromatics) than the more thermally labile OC (e.g., carbohydrates, lipids) (Sanderman and Grandy, 2020). It is also possible that methodological artefacts, such as kinetic fractionation, influenced the ^{13}C-RO contents. Kinetic fractionation is explained by different carbon isotopes evolving as CO_2 from the soil sample at different rates during the ramped heating (Hemingway et al., 2017a). Kinetic fractionation would cause the ^{13}C content of the evolved CO_2 to increase linearly with temperature (Hemingway et al., 2017a), and we cannot rule out this artefact. Hemingway et al. (2017a) determined that kinetic fractionation was not an important factor in their RPO procedure, but we used a different set-up (described in Garnett et al., 2023).

4.4. Changes in the isotopic content of ramped oxidation CO_2 fractions with depth

The isotopic composition of the evolved CO_2 did not vary significantly with depth for any of the temperature fractions. The lack of an increase in the age (^{14}C-depletion) of soil C with sample depth is unusual, as typically C undergoes a burial process, and previous work has shown diagenetic ageing of saltmarsh soils with depth as young OC is turned over faster than old OC (Komada et al., 2022; Van de Broek et al., 2018).

Compared to other UK saltmarshes, Skinflats has relatively high C accumulation rates (Miller et al., 2023; Smeaton et al., 2024). Depleted ^{14}C contents of the OC accumulating at the Skinflats saltmarsh (Houston et al., 2024b) imply that a proportion of the OC being buried may already have been aged at the time of deposition on the marsh surface, as the marsh formed in the 1930's (Miller et al., 2023). The combination of high carbon accumulation rates and depleted soil ^{14}C contents implies that the Skinflats saltmarsh accumulates a high proportion of old, most likely allochthonous OC. Some of the aged, allochthonous OC may have undergone significant microbial processing and degradation prior to its accumulation in the saltmarsh soil. As the OM is degraded, and the energetically favourable components are consumed, the resulting OM becomes increasingly thermally recalcitrant (Luk et al., 2021; Sanderman and Grandy, 2020; Soldatova et al., 2024). The accumulation of a high proportion of degraded OC on the Skinflats saltmarsh may therefore explain the lack of observed change in the isotopic composition of the soil OC pools with depth.

Not all old OC is degraded or thermally recalcitrant, and our results show that the Skinflats saltmarsh is also a store of old (^{14}C-depleted), thermally labile OC (Fig. 1). Old OC can be thermally labile if it 'ages' (is stored) in an environment with low decomposition rates, e.g., a peatland (Dean et al., 2023), prior to transport and accumulation into the saltmarsh. There are

352 extensive peatlands in the Skinflats catchment, many of which are degrading (Lilly et al., 2012).
353 Regardless of the age and degradation state of the OC deposited onto the marsh surface, as it
354 gets buried it will undergo a degree of microbial processing and degradation in the saltmarsh soil
355 (Luk et al., 2021), but that process is potentially less prevalent at Skinflats than saltmarshes
356 accumulating younger, less degraded OC.

357 Through isotopic analysis of saltmarsh soils partitioned using ramped oxidation, we have
358 determined that increased thermal recalcitrance is related to older (^{14}C-depleted; Fig. 1), more
359 degraded/microbially derived (^{13}C-enriched; Fig. 2) soil C. These findings are consistent with
360 previous research on the thermal reactivity of soil and sediment C, that more energy is required
361 (higher temperature/μE) to decompose older (^{14}C-depleted), degraded/microbially derived (^{13}C-
362 enriched) C than younger (^{14}C-enriched), less processed (^{13}C-depleted) C (e.g., Bao et al., 2019b;
363 Plante et al., 2013; Stoner et al., 2023), including one saltmarsh study (Luk et al., 2021).

364 **4.5. Comparison of biologically and thermally evolved CO_2**

365 As the biological turnover time of OC depends on the prevailing environmental conditions as well
366 as thermal reactivity (Schmidt et al., 2011), the isotopic composition of the most biologically- and
367 thermally-reactive saltmarsh soil OC pools may not be the same. To determine if this is the case,
368 or not, we compared the isotopic composition of the RO thermal reactivity fractions to the
369 isotopic composition of the CO_2 that was evolved biologically during incubations of equivalent
370 samples (Houston et al., 2024b) (Fig. 1).

371 Figure 1 shows that for each of the 0.5 cm depth samples, the ^{14}C content of the CO_2 respired in
372 the aerobic laboratory experiments was ^{14}C-enriched relative to any of the RO temperature
373 fractions, which was also the case for the T3 5.5 cm sample (Table 3). The relative ^{14}C-enrichment
374 of the biologically respired CO_2 compared to the thermally evolved CO_2 was likely caused by
375 inhomogeneity in the OC thermal reactivity pools, as each defined thermal reactivity pool may be
376 composed of multiple OC sources of variable age and composition. As thermal recalcitrance is
377 related to ^{14}C-depletion for these samples (Fig. 1), we hypothesise that for saltmarsh soil samples
378 producing respired CO_2 that was ^{14}C-enriched relative to any of the RO fractions (T1 0.5 cm, T2
379 0.5 cm, T3 0.5 cm, T3 5.5 cm; Table 1, Fig. 1), that this CO_2 was biologically-produced from an OC
380 pool within the most thermally labile RO fraction (150-325°C). Thus, we suggest that even within
381 the 150-325 °C RO fraction there are pools of even younger OC, but that they are masked by older,
382 ^{14}C-depleted OC.

383 The ^{14}C content of respired CO_2 from the 5.5 cm depth samples tended to be closer to the ^{14}C
384 content of the lowest temperature (150-325°C) RO fraction (Fig. 1), implying that for these

samples the biologically evolved CO_2 was from a thermally labile OC pool. The T2 15.5 cm respired CO_2 sample was also similar in ^{14}C content to the lowest temperature RO fraction, whereas respired CO_2 from the slightly deeper T1 18.5 cm and T3 19.5 cm samples was ^{14}C-depleted relative to the 150-325°C RO fraction, instead aligning closer to the higher temperature RO fractions (Fig. 1). The biologically evolved CO_2 from T1 18.5 cm and T3 19.5 cm was therefore not from a thermally labile OC pool. The ^{14}C content of the CO_2 evolved from the aerobic incubations of T1 18.5 cm and T3 19.5 cm was hypothesized to have been derived from an inorganic C source due to the enriched ^{13}C contents of -6.1‰ and -3.7‰, respectively (Houston et al., 2024b). As IC biological turnover times are controlled by different factors than OC (Van Dam et al., 2021), and the remainder of the samples were determined to evolve from OC substrates, this is likely to explain why the ^{14}C content of the CO_2 evolved from the aerobic incubation experiments for T1 18.5 cm and T3 19.5 cm did not align with the lowest temperature (most thermally labile) RO fraction (Fig. 1). Therefore, there was a clear depth trend in the relationship between the ^{14}C content of CO_2 respired in the aerobic incubation experiments and the ^{14}C content of RO fractions of the same bulk soils. Degradation of the thermally labile OM components to a more thermally recalcitrant state during burial may reduce the inhomogeneities within the most thermally labile RO fraction for this study.

For seven out of nine samples (T1 18.5 cm and T3 19.5 cm being the outliers), the ^{14}C content of the CO_2 evolved from the aerobic laboratory incubations was closest to the ^{14}C content of the 150-325°C RO temperature fraction. Therefore, even though the CO_2 evolved from the aerobic incubation experiments was determined to be from a predominantly aged, allochthonous OC source (Houston et al., 2024b), it can now also be shown to be derived from a predominantly thermally labile OC pool (Fig. 1).

We did not attempt to relate the ^{13}C-RO to the ^{13}C content of the CO_2 respired in the incubation experiments, due to the potential for microbial fractionation during the incubation experiments which can change the ^{13}C content of the respired CO_2 and the resulting soil OC (Soldatova et al., 2024; Werth and Kuzyakov, 2010). In contrast, ^{14}C results are normalised using the measured $\delta^{13}C$ values and are therefore immune to such isotopic fractionation effects.

4.6. Implications

Our results show that aged (presumed allochthonous), thermally labile OC stored in saltmarsh soils remains vulnerable to loss to the atmosphere upon habitat drainage. Saltmarsh soils usually exist in low-oxygen, tidally-inundated conditions which slow decomposition of OC (Chapman et al., 2019), but many saltmarshes globally have been drained (and their soils subsequently

418 oxidised) to convert them for land uses such as housing developments and agriculture (Bromberg
419 and Bertness, 2005; Campbell et al., 2022; Morris et al., 2012). In the Forth Estuary, where the
420 Skinflats saltmarsh is located, as much as 50% of the intertidal area has been converted to
421 agricultural land since 1600, often involving the drainage of saltmarshes (Hansom and
422 McGlashan, 2008).

423 Protecting saltmarshes from degradation following drainage is listed as an eligible activity for
424 generating carbon credits for blue carbon ecosystem (BCE) projects (VERRA, 2023) and there is
425 significant potential for climate mitigation by avoided emissions from protecting vulnerable
426 stocks of soil OC in BCEs (Goldstein et al., 2020; Griscom et al., 2017; Kwan et al., 2025; Sasmito
427 et al., 2025). Similarly, the re-creation of saltmarsh habitat through managed realignment
428 (rewetting by tidal inundation) of historic saltmarsh habitats which were previously reclaimed for
429 land use purposes (e.g., agriculture) could reduce (and possible reverse) the emissions of aged
430 OC to the atmosphere, both locally to Skinflats, and globally.

431 The evidence for the respiration of thermally labile, allochthonous OC from saltmarsh soils in a
432 drainage degradation scenario demonstrates that at least this fraction of allochthonous OC
433 should be counted as additional in carbon crediting projects and National GHG Inventories.
434 Because allochthonous OC can account for up to 90 % of saltmarsh soil carbon (Komada et al.,
435 2022), the inclusion of allochthonous OC (or even a fraction of it) would significantly increase the
436 climate mitigation awarded to blue carbon projects (as carbon credits, or contributions to
437 National GHG Inventories) (Houston et al., 2024a).

438 As the bioavailable OC respired in the experiments of Houston et al. (2024b) was (in most cases)
439 from a predominantly thermally labile OC pool, and ^{14}C-RO decreased (C became older) with
440 increasing temperature (thermal recalcitrance), RO measurements could be useful for
441 characterising the turnover times of OC pools for saltmarsh soils exposed to oxic conditions
442 (drainage degradation scenario). The use of thermally defined OC pools to characterize OC
443 turnover times for saltmarsh soils would require a modelling advancement to constrain
444 degradation rates and residence times. Such efforts are not within the scope of this study but
445 could inform additionality/permanence in these saltmarsh systems. Experimentally defined
446 turnover times of OC thermal reactivity pools could, for example, provide a more robust approach
447 than inclusion/exclusion of allochthonous OC from saltmarsh 'blue carbon' projects (Houston et
448 al., 2024a).

449 Further research is needed to determine if the relationship between biological and thermal
450 lability exists for different degradation scenarios such as nutrient enrichment, as OC turnover

time depends on the environmental conditions as well as the thermal lability of the OC pools. Similarly, these experiments would need to be replicated for a wider range of saltmarshes (high and low latitude saltmarshes, different typologies), as there are likely to be differences in OC turnover in different systems.

The samples used for this study were from the low marsh zone only, but it is likely that the thermal reactivity of the Skinflats saltmarsh soil C will vary spatially across the marsh, as the proportion of OC sources has been shown to be variable across saltmarshes (Middelburg et al., 1997). Given our findings that old (^{14}C-depleted) OC has greater thermal recalcitrance than young (^{14}C-enriched) OC (Fig. 1), we anticipate that higher marsh zones, which typically have greater proportions of autochthonous OC than lower marsh zones (Spohn et al., 2013), would contain a greater proportion of thermally labile OC. However, it is important to recognise that some of the young (^{14}C-enriched), autochthonous OC in saltmarsh soils can also be thermally recalcitrant. As well as marsh zonation, we expect that the proportion of OC sources (and associated mix of thermal reactivities) would also vary with proximity to marsh creeks which redistribute autochthonous and allochthonous C across the saltmarsh habitat (Middelburg et al., 1997; Reed et al., 1999). In previously published work we showed that Skinflats accumulates OC of a much greater 'age' (depleted soil ^{14}C contents) than two other saltmarshes in Scotland (Houston et al., 2024b).

In this paper we have determined that age (^{14}C-content) is related to the thermal recalcitrance of saltmarsh soil OC. We therefore speculate that sites accumulating younger OC would have more thermally labile soil OC than sites accumulating older OC, like Skinflats, with wider implications for the risks to these vulnerable stores of soil carbon from human disturbances.

5. Conclusions

This is the first study on saltmarsh soils to employ the ramped oxidation method. We show that old (^{14}C-depleted) carbon dominates the thermally recalcitrant OC pools. The thermally labile OC pools are also aged (^{14}C-depleted) compared to the contemporary atmosphere but are younger than the thermally recalcitrant OC pools. These results highlight the role of saltmarshes as mixed stores of both old, thermally recalcitrant OC, as well as younger, thermally labile OC.

We present the first comparison of the bioavailability (CO_2 evolved from incubation experiments; Houston et al., 2024)) and the thermal reactivity (RO) of saltmarsh soil OC. We show that aged, allochthonous CO_2 evolved from saltmarsh soils exposed to oxic conditions (Houston et al., 2024b) are from a predominantly thermally labile OC pool. As saltmarsh soils exist mostly in low

oxygen, waterlogged conditions, management interventions to limit their exposure to elevated oxygen availability may protect and conserve these stores of thermally labile OC and provide a climate abatement service. Therefore, we recommend that thermally labile allochthonous OC stored in saltmarsh soils should be counted as additional in some carbon crediting projects and National GHG Inventories.

Appendix A

Table A1. Additional ^{14}C measurement from the 650-800 °C. ^{14}C was measured at the Scottish Universities Environmental Research Centre Accelerator Mass Spectrometer (AMS) Laboratory. $\delta^{13}C$ (relative to Vienna PDB standard) was measured using isotope ratio mass spectrometry on a Delta V (Thermo, Germany) and used to normalize the ^{14}C results to a $\delta^{13}C = -25‰$, which were reported as %Modern ^{14}C (i.e., Fraction modern × 100). Errors are reported to one standard deviation from the mean.

Sample ID	% Modern ^{14}C
Skin T1 0.5 cm 650-800 °C	79.75 ± 0.50

Table A2. Isotopic compositions measured by IRMS ($\delta^{13}C$) compared to values estimated by the rampedpyrox model (Hemingway, 2016). Modelled and measured $\delta^{13}C$ values are significantly different (Mann-Whittney-U test, p = 0.04).

Sample ID	$\delta^{13}C$ (measured)	$\delta^{13}C$ (modelled)
Skin T1 0-1cm 150-325 °C	-24.7 ± 0.1	-30.1 ± 0.2
Skin T1 0-1cm 325-425 °C	-22.3 ± 0.1	-27.8 ± 0.2
Skin T1 0-1cm 425-500 °C	-20.2 ± 0.1	-25.6 ± 0.2
Skin T1 0-1cm 500-650 °C	-13.9 ± 0.1	-19.5 ± 0.2
Skin T1 0-1cm 650-800 °C	-5.6 ± 0.1	-11.1 ± 0.2
Skin T1 5-6cm 150-325 °C	-26.7 ± 0.1	-27.7 ± 0.2
Skin T1 5-6cm 325-425 °C	-24.7 ± 0.1	-25.8 ± 0.2
Skin T1 5-6cm 425-500 °C	-22.7 ± 0.1	-23.8 ± 0.2
Skin T1 5-6cm 500-650 °C	-21.3 ± 0.1	-22.6 ± 0.2
Skin T1 5-6cm 650-800 °C	-6.3 ± 0.1	-8.0 ± 0.2
Skin T1 18-19cm 150-325 °C	-25.9 ± 0.1	-27.3 ± 0.2
Skin T1 18-19cm 325-425 °C	-24.0 ± 0.1	-25.4 ± 0.2
Skin T1 18-19cm 425-500 °C	-22.6 ± 0.1	-24.1 ± 0.2
Skin T1 18-19cm 500-650 °C	-21.6 ± 0.1	-23.3 ± 0.2
Skin T1 18-19cm 650-800 °C	-9.5 ± 0.1	-11.0 ± 0.2
Skin T2 0-1cm 150-325 °C	-25.7 ± 0.1	-27.9 ± 0.2
Skin T2 0-1cm 325-425 °C	-23.6 ± 0.1	-25.9 ± 0.2
Skin T2 0-1cm 425-500 °C	-22.0 ± 0.1	-24.3 ± 0.2
Skin T2 0-1cm 500-650 °C	-19.9 ± 0.1	-22.4 ± 0.2
Skin T2 0-1cm 650-800 °C	-4.7 ± 0.1	-7.2 ± 0.2
Skin T2 5-6cm 150-325 °C	-26.5 ± 0.1	-27.4 ± 0.2
Skin T2 5-6cm 325-425 °C	-24.8 ± 0.1	-25.8 ± 0.2
Skin T2 5-6cm 425-500 °C	-23.0 ± 0.1	-24.0 ± 0.2
Skin T2 5-6cm 500-650 °C	-22.0 ± 0.1	-23.1 ± 0.2

Skin T2 5-6cm 650-800 °C	-21.1 ± 0.1	-22.3 ± 0.2
Skin T2 15-16cm 150-325 °C	-28.0 ± 0.1	-26.9 ± 0.2
Skin T2 15-16cm 325-425 °C	-26.6 ± 0.1	-25.5 ± 0.2
Skin Tr2 15-16cm 425-500 °C	-25.4 ± 0.1	-24.3 ± 0.2
Skin Tr2 15-16cm 500-650 °C	-24.4 ± 0.1	-23.6 ± 0.2
Skin T2 15-16cm 650-800 °C	-4.0 ± 0.1	-2.9 ± 0.2
Skin T3 0-1cm 150-325 °C	-25.3 ± 0.1	-27.3 ± 0.2
Skin T3 0-1cm 325-425 °C	-23.7 ± 0.1	-25.7 ± 0.2
Skin T3 0-1cm 425-500 °C	-22.0 ± 0.1	-24.1 ± 0.2
Skin T3 0-1cm 500-650 °C	-18.7 ± 0.1	-21.0 ± 0.2
Skin T3 0-1cm 650-800 °C	-4.1 ± 0.1	-6.2 ± 0.2
Skin T3 5-6cm 150-325 °C	-26.2 ± 0.1	-27.8 ± 0.2
Skin T3 5-6cm 325-425 °C	-24.2 ± 0.1	-25.9 ± 0.2
Skin T3 5-6cm 425-500 °C	-22.6 ± 0.1	-24.3 ± 0.2
Skin T3 5-6cm 500-650 °C	-20.50 ± 0.1	-22.32 ± 0.2
Skin T3 5-6cm 650-800 °C	-12.60 ± 0.1	-14.29 ± 0.2
Skin T3 19-20cm 150-325 °C	-26.30 ± 0.1	-27.48 ± 0.2
Skin T3 19-20cm 325-425 °C	-24.20 ± 0.1	-25.40 ± 0.2
Skin T3 19-20cm 425-500 °C	-22.60 ± 0.1	-23.78 ± 0.2
Skin T3 19-20cm 500-650 °C	-21.20 ± 0.1	-22.57 ± 0.2
Skin T3 19-20cm 650-800 °C	-8.00 ± 0.1	-9.30 ± 0.2

Table A3. Soil carbon properties measured on equivalent sub-samples prior to the RO procedure, as reported in Houston et al. (2024). Total organic carbon (TOC), Total carbon (TC) for the soil samples were measured by a SoliTOC analyser (Elementar Analysensysteme, Hanau, Germany). ^{14}C was measured at the Scottish Universities Environmental Research Centre Accelerator Mass Spectrometer (AMS) Laboratory. $\delta^{13}C$ (relative to Vienna PDB standard) was measured using isotope ratio mass spectrometry on a Delta V (Thermo, Germany) and used to normalize the ^{14}C results to a $\delta^{13}C = -25‰$, which were reported as %Modern ^{14}C (i.e., Fraction modern × 100). Errors are reported to one standard deviation from the mean.

Sample ID	TOC (%)	TIC (%)	TC (%)	% Modern ^{14}C	$\delta^{13}C$
SK T1 0.5 cm	4.1	0.48	4.58	47.49 ± 0.23	-23.5 ± 0.1
SK T1 5.5 cm	4.96	0.11	5.06	45.03 ± 0.20	-24.5 ± 0.1
SK T1 18.5 cm	4.8	0.39	5.18	41.36 ± 0.19	-23.8 ± 0.1
SK T2 0.5 cm	4.71	0.16	4.87	31.47 ± 0.15	-22.2 ± 0.1
SK T2 5.5 cm	4.23	0.13	4.36	43.69 ± 0.21	-24.1 ± 0.1
SK T2 15.5 cm	7.56	0.15	7.71	50.93 ± 0.24	-25.1 ± 0.1
SK T3 0.5 cm	5.37	0.12	5.49	47.03 ± 0.22	-23.7 ± 0.1
SK T3 5.5 cm	4.06	0.11	4.18	44.15 ± 0.21	24.0 ± 0.1
SK T3 19.5 cm	5.23	0.12	5.35	44.48 ± 0.21	-24.1 ± 0.1

Data Availability

All data presented in this manuscript is available in the main text and appendices.

Author Contribution Statement

A.H. undertook the study, fieldwork, sample processing, data acquisition, and wrote the first draft of the manuscript. M.G. conducted the laboratory procedures with the help of A.H. A.H., W.A., and M.G. contributed to designing the study, fieldwork, and laboratory analyses. W.A., M.G., and J.S. oversaw the study and contributed to writing and revision of the manuscript.

Competing Interests

The authors declare that they have no conflict of interest.

Acknowledgements

We thank Jo Smith (University of Aberdeen) for her comments and edits on the first draft of this manuscript. We thank the NERC SUPER DTP for funding the PhD through which this research was undertaken (NE/S007342/1). We acknowledge support from the National Environmental Isotope Facility in funding the ^{14}C measurements for this study under grant NE/S011587/1 (allocation numbers 2594.1022, 2709.1023). WENA also acknowledges support provided by the HORIZON-CL5-2023-D1-02-02 grant C-BLUES, Innovation to advance the evidence base for reporting of Blue Carbon inventories and greenhouse gas fluxes in coastal wetlands. Thanks are extended to Chloe Bates for assisting with sample collection. Finally, we thank the editor and both reviewers for their comments which have improved this manuscript.

Reference List

Ascough, P., Bompard, N., Garnett, M. H., Gulliver, P., Murray, C., Newton, J.-A., and Taylor, C.: 14C measurement of samples for environmental science applications at the National Environmental Isotope Facility (NEIF) Radiocarbon Laboratory, SUERC, UK, Radiocarbon, 66, 1020–1031, https://doi.org/10.1017/RDC.2024.9, 2024.

Bao, R., McNichol, A. P., Hemingway, J. D., Gaylord, M. C. L., and Eglinton, T. I.: Influence of Different Acid Treatments on the Radiocarbon Content Spectrum of Sedimentary Organic Matter Determined by RPO/Accelerator Mass Spectrometry, Radiocarbon, 61, 395–413, https://doi.org/10.1017/RDC.2018.125, 2019a.

Bao, R., Zhao, M., McNichol, A., Wu, Y., Guo, X., Haghipour, N., and Eglinton, T. I.: On the Origin of Aged Sedimentary Organic Matter Along a River-Shelf-Deep Ocean Transect, Journal of Geophysical Research: Biogeosciences, 124, 2582–2594, https://doi.org/10.1029/2019JG005107, 2019b.

Bianchi, T. S., Mayer, L. M., Amaral, J. H. F., Arndt, S., Galy, V., Kemp, D. B., Kuehl, S. A., Murray, N. J., and Regnier, P.: Anthropogenic impacts on mud and organic carbon cycling, Nat. Geosci., 1–11, https://doi.org/10.1038/s41561-024-01405-5, 2024.

Boström, B., Comstedt, D., and Ekblad, A.: Isotope fractionation and 13C enrichment in soil profiles during the decomposition of soil organic matter, Oecologia, 153, 89–98, https://doi.org/10.1007/s00442-007-0700-8, 2007.

Brand, W. A., Coplen, T. B., Vogl, J., Rosner, M., and Prohaska, T.: Assessment of international reference materials for isotope-ratio analysis (IUPAC Technical Report), Pure and Applied Chemistry, 86, 425–467, https://doi.org/10.1515/pac-2013-1023, 2014.

Bromberg, K. D. and Bertness, M. D.: Reconstructing New England salt marsh losses using historical maps, Estuaries, 28, 823–832, https://doi.org/10.1007/BF02696012, 2005.

Campbell, A. D., Fatoyinbo, L., Goldberg, L., and Lagomasino, D.: Global hotspots of salt marsh change and carbon emissions, Nature, 1–6, https://doi.org/10.1038/s41586-022-05355-z, 2022.

Chapman, S. K., Hayes, M. A., Kelly, B., and Langley, J. A.: Exploring the oxygen sensitivity of wetland soil carbon mineralization, Biology Letters, 15, 20180407, https://doi.org/10.1098/rsbl.2018.0407, 2019.

Dean, J. F., Billett, M. F., Turner, T. E., Garnett, M. H., Andersen, R., McKenzie, R. M., Dinsmore, K. J., Baird, A. J., Chapman, P. J., and Holden, J.: Peatland pools are tightly coupled to the contemporary carbon cycle, Global Change Biology, n/a, e16999, https://doi.org/10.1111/gcb.16999, 2023.

Etcheverría, P., Huygens, D., Godoy, R., Borie, F., and Boeckx, P.: Arbuscular mycorrhizal fungi contribute to 13C and 15N enrichment of soil organic matter in forest soils, Soil Biology and Biochemistry, 41, 858–861, https://doi.org/10.1016/j.soilbio.2009.01.018, 2009.

Garnett, M. H., Pereira, R., Taylor, C., Murray, C., and Ascough, P. L.: A New Ramped Oxidation-14C Analysis Facility at the NEIF Radiocarbon Laboratory, East Kilbride, UK, Radiocarbon, 65, 1213–1229, https://doi.org/10.1017/RDC.2023.96, 2023.

Geraldi, N. R., Ortega, A., Serrano, O., Macreadie, P. I., Lovelock, C. E., Krause-Jensen, D., Kennedy, H., Lavery, P. S., Pace, M. L., Kaal, J., and Duarte, C. M.: Fingerprinting Blue Carbon: Rationale and Tools to Determine the Source of Organic Carbon in Marine Depositional Environments, Frontiers in Marine Science, 6, 263, https://doi.org/10.3389/fmars.2019.00263, 2019.

Goldstein, A., Turner, W. R., Spawn, S. A., Anderson-Teixeira, K. J., Cook-Patton, S., Fargione, J., Gibbs, H. K., Griscom, B., Hewson, J. H., Howard, J. F., Ledezma, J. C., Page, S., Koh, L. P., Rockström, J., Sanderman, J., and Hole, D. G.: Protecting irrecoverable carbon in Earth's ecosystems, Nat. Clim. Chang., 10, 287–295, https://doi.org/10.1038/s41558-020-0738-8, 2020.

Granse, D., Wanner, A., Stock, M., Jensen, K., and Mueller, P.: Plant-sediment interactions decouple inorganic from organic carbon stock development in salt marsh soils, Limnology and Oceanography Letters, n/a, https://doi.org/10.1002/lol2.10382, 2024.

Griscom, B. W., Adams, J., Ellis, P. W., Houghton, R. A., Lomax, G., Miteva, D. A., Schlesinger, W. H., Shoch, D., Siikamäki, J. V., Smith, P., Woodbury, P., Zganjar, C., Blackman, A., Campari, J., Conant, R. T., Delgado, C., Elias, P., Gopalakrishna, T., Hamsik, M. R., Herrero, M., Kiesecker, J., Landis, E., Laestadius, L., Leavitt, S. M., Minnemeyer, S., Polasky, S., Potapov, P., Putz, F. E., Sanderman, J., Silvius, M., Wollenberg, E., and Fargione, J.: Natural climate solutions, Proceedings of the National Academy of Sciences, 114, 11645–11650, https://doi.org/10.1073/pnas.1710465114, 2017.

Hajdas, I., Ascough, P., Garnett, M. H., Fallon, S. J., Pearson, C. L., Quarta, G., Spalding, K. L., Yamaguchi, H., and Yoneda, M.: Radiocarbon dating, Nat Rev Methods Primers, 1, 1–26, https://doi.org/10.1038/s43586-021-00058-7, 2021.

Hemingway, J. D.: rampedpyrox: Open-source tools for thermoanalytical data analysis, 2016-, 2016.

Hemingway, J. D., Galy, V. V., Gagnon, A. R., Grant, K. E., Rosengard, S. Z., Soulet, G., Zigah, P. K., and McNichol, A. P.: Assessing the Blank Carbon Contribution, Isotope Mass Balance, and Kinetic Isotope Fractionation of the Ramped Pyrolysis/Oxidation Instrument at NOSAMS, Radiocarbon, 59, 179–193, https://doi.org/10.1017/RDC.2017.3, 2017a.

Hemingway, J. D., Rothman, D. H., Rosengard, S. Z., and Galy, V. V.: Technical note: An inverse method to relate organic carbon reactivity to isotope composition from serial oxidation, Biogeosciences, 14, 5099–5114, https://doi.org/10.5194/bg-14-5099-2017, 2017b.

Hemingway, J. D., Rothman, D. H., Grant, K. E., Rosengard, S. Z., Eglinton, T. I., Derry, L. A., and Galy, V. V.: Mineral protection regulates long-term global preservation of natural organic carbon, Nature, 570, 228–231, https://doi.org/10.1038/s41586-019-1280-6, 2019.

Houston, A., Kennedy, H., and Austin, W. E. N.: Additionality in Blue Carbon Ecosystems: Recommendations for a Universally Applicable Accounting Methodology, Global Change Biology, 30, e17559, https://doi.org/10.1111/gcb.17559, 2024a.

Houston, A., Garnett, M. H., and Austin, W. E. N.: Blue carbon additionality: New insights from the radiocarbon content of saltmarsh soils and their respired CO2, Limnology and Oceanography, n/a, https://doi.org/10.1002/lno.12508, 2024b.

Howard, J., Sutton-Grier, A. E., Smart, L. S., Lopes, C. C., Hamilton, J., Kleypas, J., Simpson, S., McGowan, J., Pessarrodona, A., Alleway, H. K., and Landis, E.: Blue carbon pathways for climate mitigation: Known, emerging and unlikely, Marine Policy, 156, 105788, https://doi.org/10.1016/j.marpol.2023.105788, 2023.

Komada, T., Bravo, A., Brinkmann, M.-T., Lu, K., Wong, L., and Shields, G.: “Slow” and “fast” in blue carbon: Differential turnover of allochthonous and autochthonous organic matter in minerogenic salt marsh sediments, Limnology and Oceanography, n/a, https://doi.org/10.1002/lno.12090, 2022.

Kwan, V., Friess, D. A., Sarira, T. V., and Zeng, Y.: Permanence risks limit blue carbon financing strategies to safeguard Southeast Asian mangroves, Commun Earth Environ, 6, 1–8, https://doi.org/10.1038/s43247-025-02035-4, 2025.

Leng, M. J. and Lewis, J. P.: C/N ratios and Carbon Isotope Composition of Organic Matter in Estuarine Environments, in: Applications of Paleoenvironmental Techniques in Estuarine Studies, edited by: Weckström, K., Saunders, K. M., Gell, P. A., and Skilbeck, C. G., Springer Netherlands, Dordrecht, 213–237, https://doi.org/10.1007/978-94-024-0990-1_9, 2017.

Lilly, A., Baggaley, N., and Donnelly, D.: Map of soil organic carbon in top soils of Scotland, 2012.

Luk, S. Y., Todd-Brown, K., Eagle, M., McNichol, A. P., Sanderman, J., Gosselin, K., and Spivak, A. C.: Soil Organic Carbon Development and Turnover in Natural and Disturbed Salt Marsh Environments, Geophysical Research Letters, 48, e2020GL090287, https://doi.org/10.1029/2020GL090287, 2021.

628 Macreadie, P. I., Anton, A., Raven, J. A., Beaumont, N., Connolly, R. M., Friess, D. A., Kelleway, J.
629 J., Kennedy, H., Kuwae, T., Lavery, P. S., Lovelock, C. E., Smale, D. A., Apostolaki, E. T., Atwood, T.
630 B., Baldock, J., Bianchi, T. S., Chmura, G. L., Eyre, B. D., Fourqurean, J. W., Hall-Spencer, J. M.,
631 Huxham, M., Hendriks, I. E., Krause-Jensen, D., Laffoley, D., Luisetti, T., Marbà, N., Masque, P.,
632 McGlathery, K. J., Megonigal, J. P., Murdiyarso, D., Russell, B. D., Santos, R., Serrano, O.,
633 Silliman, B. R., Watanabe, K., and Duarte, C. M.: The future of Blue Carbon science, Nature
634 Communications, 10, 3998, https://doi.org/10.1038/s41467-019-11693-w, 2019.

635 Macreadie, P. I., Costa, M. D. P., Atwood, T. B., Friess, D. A., Kelleway, J. J., Kennedy, H.,
636 Lovelock, C. E., Serrano, O., and Duarte, C. M.: Blue carbon as a natural climate solution, Nat
637 Rev Earth Environ, 2, 826–839, https://doi.org/10.1038/s43017-021-00224-1, 2021.

638 Middelburg, J. J., Nieuwenhuize, J., Lubberts, R. K., and van de Plassche, O.: Organic Carbon
639 Isotope Systematics of Coastal Marshes, Estuarine, Coastal and Shelf Science, 45, 681–687,
640 https://doi.org/10.1006/ecss.1997.0247, 1997.

641 Miller, L. C., Smeaton, C., Yang, H., and Austin, W. E. N.: Carbon accumulation and storage
642 across contrasting saltmarshes of Scotland, Estuarine, Coastal and Shelf Science, 108223,
643 https://doi.org/10.1016/j.ecss.2023.108223, 2023.

644 Morris, J. T., Edwards, J., Crooks, S., and Reyes, E.: Assessment of carbon sequestration
645 potential in coastal wetlands, in: Recarbonization of the Biosphere: Ecosystems and the Global
646 Carbon Cycle, 517–532, https://doi.org/10.1007/978-94-007-4159-1_24, 2012.

647 Noyce, G. L., Smith, A. J., Kirwan, M. L., Rich, R. L., and Megonigal, J. P.: Oxygen priming induced
648 by elevated CO2 reduces carbon accumulation and methane emissions in coastal wetlands,
649 Nat. Geosci., 16, 63–68, https://doi.org/10.1038/s41561-022-01070-6, 2023.

650 Peltre, C., Fernández, J. M., Craine, J. M., and Plante, A. F.: Relationships between Biological and
651 Thermal Indices of Soil Organic Matter Stability Differ with Soil Organic Carbon Level, Soil
652 Science Society of America Journal, 77, 2020–2028, https://doi.org/10.2136/sssaj2013.02.0081,
653 2013.

654 Plante, A. F., Fernández, J. M., Haddix, M. L., Steinweg, J. M., and Conant, R. T.: Biological,
655 chemical and thermal indices of soil organic matter stability in four grassland soils, Soil Biology
656 and Biochemistry, 43, 1051–1058, https://doi.org/10.1016/j.soilbio.2011.01.024, 2011.

657 Plante, A. F., Beaupré, S. R., Roberts, M. L., and Baisden, T.: Distribution of Radiocarbon Ages in
658 Soil Organic Matter by Thermal Fractionation, Radiocarbon, 55, 1077–1083,
659 https://doi.org/10.1017/S0033822200058215, 2013.

660 R Core Team: R: A language and environment for statistical computing., 2022.

661 Ramnarine, R., Wagner-Riddle, C., Dunfield, K. E., and Voroney, R. P.: Contributions of
662 carbonates to soil CO2 emissions, Can. J. Soil. Sci., 92, 599–607,
663 https://doi.org/10.4141/cjss2011-025, 2012.

664 Reed, D. J., Spencer, T., Murray, A. L., French, J. R., and Leonard, L.: Marsh surface sediment
665 deposition and the role of tidal creeks: Implications for created and managed coastal marshes,
666 J Coast Conserv, 5, 81–90, https://doi.org/10.1007/BF02802742, 1999.

667 Rosenheim, B. E., Day, M. B., Domack, E., Schrum, H., Benthien, A., and Hayes, J. M.: Antarctic
668 sediment chronology by programmed-temperature pyrolysis: Methodology and data treatment,
669 Geochemistry, Geophysics, Geosystems, 9, https://doi.org/10.1029/2007GC001816, 2008.

670 Saintilan, N., Rogers, K., Mazumder, D., and Woodroffe, C.: Allochthonous and autochthonous
671 contributions to carbon accumulation and carbon store in southeastern Australian coastal
672 wetlands, Estuarine, Coastal and Shelf Science, 128, 84–92,
673 https://doi.org/10.1016/j.ecss.2013.05.010, 2013.

674 Sanderman, J. and Grandy, A. S.: Ramped thermal analysis for isolating biologically meaningful
675 soil organic matter fractions with distinct residence times, SOIL, 6, 131–144,
676 https://doi.org/10.5194/soil-6-131-2020, 2020.

677 Sasmito, S. D., Taillardat, P., Adinugroho, W. C., Krisnawati, H., Novita, N., Fatoyinbo, L., Friess,
678 D. A., Page, S. E., Lovelock, C. E., Murdiyarso, D., Taylor, D., and Lupascu, M.: Half of land use
679 carbon emissions in Southeast Asia can be mitigated through peat swamp forest and mangrove
680 conservation and restoration, Nat Commun, 16, 740, https://doi.org/10.1038/s41467-025-
681 55892-0, 2025.

682 Schmidt, M. W. I., Torn, M. S., Abiven, S., Dittmar, T., Guggenberger, G., Janssens, I. A., Kleber,
683 M., Kögel-Knabner, I., Lehmann, J., Manning, D. A. C., Nannipieri, P., Rasse, D. P., Weiner, S., and
684 Trumbore, S. E.: Persistence of soil organic matter as an ecosystem property, Nature, 478, 49–
685 56, https://doi.org/10.1038/nature10386, 2011.

686 Smeaton, C., Garrett, E., Koot, M. B., Ladd, C. J. T., Miller, L. C., McMahon, L., Foster, B., Barlow,
687 N. L. M., Blake, W., Gehrels, W. R., Skov, M. W., and Austin, W. E. N.: Organic carbon
688 accumulation in British saltmarshes, Science of The Total Environment, 926, 172104,
689 https://doi.org/10.1016/j.scitotenv.2024.172104, 2024.

690 Soldatova, E., Krasilnikov, S., and Kuzyakov, Y.: Soil organic matter turnover: Global implications
691 from δ13C and δ15N signatures, Science of The Total Environment, 912, 169423,
692 https://doi.org/10.1016/j.scitotenv.2023.169423, 2024.

693 Spivak, A. C., Sanderman, J., Bowen, J. L., Canuel, E. A., and Hopkinson, C. S.: Global-change
694 controls on soil-carbon accumulation and loss in coastal vegetated ecosystems, Nat. Geosci.,
695 12, 685–692, https://doi.org/10.1038/s41561-019-0435-2, 2019.

696 Spohn, M., Babka, B., and Giani, L.: Changes in soil organic matter quality during sea-influenced
697 marsh soil development at the North Sea coast, CATENA, 107, 110–117,
698 https://doi.org/10.1016/j.catena.2013.02.006, 2013.

699 Stoner, S. W., Schrumpf, M., Hoyt, A., Sierra, C. A., Doetterl, S., Galy, V., and Trumbore, S.: How
700 well does ramped thermal oxidation quantify the age distribution of soil carbon? Assessing
701 thermal stability of physically and chemically fractionated soil organic matter, Biogeosciences,
702 20, 3151–3163, https://doi.org/10.5194/bg-20-3151-2023, 2023.

703 Van Dam, B. R., Zeller, M. A., Lopes, C., Smyth, A. R., Böttcher, M. E., Osburn, C. L., Zimmerman,
704 T., Pröfrock, D., Fourqurean, J. W., and Thomas, H.: Calcification-driven CO2 emissions exceed
705 “Blue Carbon” sequestration in a carbonate seagrass meadow, Science Advances, 7, eabj1372,
706 https://doi.org/10.1126/sciadv.abj1372, 2021.

707 Van de Broek, M., Vandendriessche, C., Poppelmonde, D., Merckx, R., Temmerman, S., and
708 Govers, G.: Long-term organic carbon sequestration in tidal marsh sediments is dominated by

old-aged allochthonous inputs in a macrotidal estuary, Global Change Biology, 24, 2498–2512, https://doi.org/10.1111/gcb.14089, 2018.

VERRA: VM0033 Methodology for Tidal Wetland and Seagrass Restoration, v2.1, 2023.

Werth, M. and Kuzyakov, Y.: 13C fractionation at the root–microorganisms–soil interface: A review and outlook for partitioning studies, Soil Biology and Biochemistry, 42, 1372–1384, https://doi.org/10.1016/j.soilbio.2010.04.009, 2010.

Williams, E. K. and Rosenheim, B. E.: What happens to soil organic carbon as coastal marsh ecosystems change in response to increasing salinity? An exploration using ramped pyrolysis, Geochemistry, Geophysics, Geosystems, 16, 2322–2335, https://doi.org/10.1002/2015GC005839, 2015.